Hindawi
Journal of Chemistry
Volume 2017, Article ID 2163608, 6 pages
https://doi.org/10.1155/2017/2163608

Research Article

UV Photocatalytic Activity for Water Decomposition of $Sr_xBa_{1-x}Nb_2O_6$ Nanocrystals with Different Components and Morphologies

Guoqiang Han,[1,2] Shuguang Cao,[1] and Bo Lin[1]

[1] *School of Mechanical Engineering and Automation, Fuzhou University, Fuzhou, Fujian 350108, China*
[2] *Fujian Institute of Research on the Structure of Matter, Chinese Academy of Science, Fuzhou, Fujian 350002, China*

Correspondence should be addressed to Guoqiang Han; galehan@hotmail.com

Received 28 January 2017; Revised 25 April 2017; Accepted 15 May 2017; Published 5 June 2017

Academic Editor: Roberto Comparelli

Strontium barium niobate $Sr_xBa_{1-x}Nb_2O_6$ (SBN) nanocrystals with different components (x = 0.2, 0.4, 0.6, and 0.8) were synthesized by Molten Salt Synthesis (MSS) method at various reaction temperatures (T = 950°C, 1000°C, 1050°C, and 1100°C). The SBN nanocrystals yielded through flux reactions possess different morphologies and sizes with a length of about ~100 nm~7 μm and a diameter of about ~200~500 nm. The Scanning Electron Microscopy (SEM) and X-ray Diffraction (XRD) techniques were used to study the compositions, structures, and morphologies of the nanocrystals. The absorption edges of the SBN nanocrystals are at a wavelength region of approximate 390 nm, which corresponds to band-gap energy of ~3.18 eV. The SBN nanocrystals with different sizes display different photocatalytic activity under ultraviolet light in decomposition of water. The SBN60 nanocrystals exhibit stable photocatalytic rates (~100~130 μmol of $H_2 \cdot g^{-1} \cdot h^{-1}$) for hydrogen production. The SBN nanocrystals can be a potential material in the application of photocatalysis and micro/nanooptical devices.

1. Introduction

The synthesis of nanostructures has attracted extensive attention in the past two decades due to their novel size-dependent properties. The SBN nanocrystals have a complex structure of tetragonal tungsten-bronze with NbO_6 octahedrons [1]. The strontium barium niobate $Sr_xBa_{1-x}Nb_2O_6$ (SBN) nanocrystals have exhibited a variety of ferroelectricity [2–4], photorefractive [5], electrooptic, nonlinear optical [1, 6], and thermoelectric properties [7] which are potentially important for many applications in various fields. The advantage of SBN nanocrystals is generally attractive for some device applications, such as thin film devices [2], optical sensors [8], and piezoelectric ceramic resonators [9]. In addition, SBN nanocrystals have lead-free composition which is concerned with environment, safety, and health. SBN nanocrystals with varied compositions can be fabricated into different sizes and complex shapes through low-cost and easy methods such as template-assisted synthesis and template-free synthesis, Czochralski method, dual-stage sintering method, and low-temperature combustion synthesis process [10–13]. The conventional SBN ferroelectric thin films are usually crystallized at the temperature of about 700~800°C and the SBN nanocrystals can be synthesized at the temperature of about 1100°C [14–16].

The hydrogen generation through splitting of water has been a topic of severely popular research interest because it is considered to be a promising method of providing renewable energy. Hydrogen energy is increasingly becoming significant from the viewpoint of both solar energy employment and environment, particularly in the case of the exhaustion of fossil fuels. Furthermore, the combustion product of hydrogen is water which has less pollution to the environment than other organic fuels. Many materials have been used as catalysts for photochemical decomposition of water, such as $Na_2Ta_4O_{11}$, $Ba_5Nb_4O_{15}$, MgO-ZrO_2, and $Sr_2Nb_2O_7$ [17–21]. However, SBN nanocrystals have received very little attention in this area. The morphology of nano-crystal has an important effect on the performance of photocatalytic. As stimulated by the promising photocatalytic and optical application, the

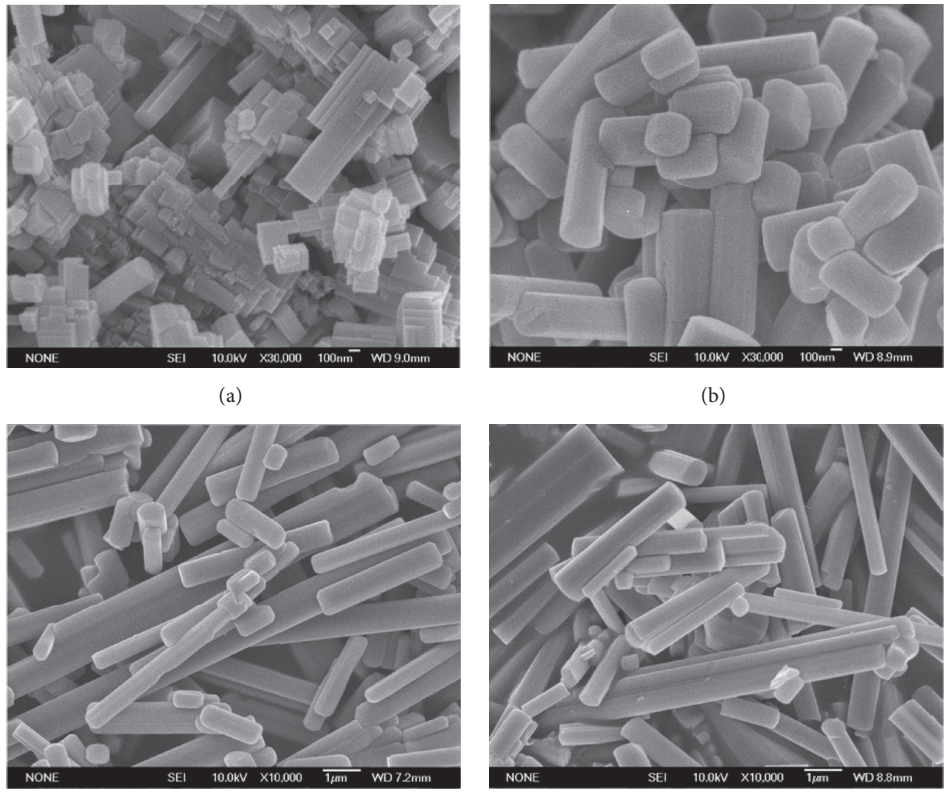

Figure 1: SEM images of the flux-synthesized SBN nanocrystals with flux-to-reactant weight ratio of 2 : 1 at a reaction temperature of 1100°C for 3 h: (a) SBN20, (b) SBN40, (c) SBN60, and (d) SBN80.

synthesis of more efficient light-driven SBN nanocrystals with complex morphologies is a subject of considerable research interest.

2. Experimental

$Sr_xBa_{1-x}Nb_2O_6$ (SBN) nanocrystals with $x = 0.2$, 0.4, 0.6, and 0.8 were prepared from molten NaCl salts (hereafter abbreviated as SBN20, etc.). The starting powders of $SrCO_3$, $BaCO_3$, and Nb_2O_5 were premixed according to the desired Sr : Ba : Nb ratios in ethanol for 24 h. The mixtures were again mixed with NaCl for 8 h, with the weight ratio of oxides to salts being equal to 1 : 2. The final mixtures of powders and salts were heated in covered high alumina crucibles for Molten Salt Synthesis (MSS). The mixtures were heated at 950°C, 1000°C, 1050°C, and 1100°C, respectively for 3 h. The nanocrystals were collected after washing away the remaining salt with hot deionized water.

The SBN nanocrystals were characterized by powder X-Ray Diffraction (XRD, Ultima-IV, Rigaku, Japan), Scanning Electron Microscopy (SEM, JSM6700-F, JEOL, Japan), and UV-vis Diffraction Reflected Spectra (DRS, Lambda900, PerkinElmer, USA). The surface area measurements were performed with laser Particle Size and Zeta Potential Analyzer (PSZPA, BI-200SM, BROOKHAVEN, USA). The photocatalytic reaction was carried out in a gas-closed circulation system. The sample of 0.05 g was dispersed in 50 ml of solution in an irradiation cell of volume 100 cm^3 quartz reactor and was illuminated with 400 W Hg lamp. The solution was stirred for 30 mins in the dark to obtain a good dispersion of the catalyst in water. The net balanced photocatalytic reaction (under irradiation) is $H_2O \rightarrow H_2 + 1/2O_2$. The evolved H_2 and O_2 were separated with molecular sieve-5 Å column and the amount of gas was determined by using gas chromatography with thermal conductivity detector.

3. Results and Discussion

These SBN nanocrystals were found to have rod-like shapes with the length of ~100 nm~7 μm and the diameter of ~200~500 nm as shown in Figures 1 and 2. Figure 1 shows the SEM images of the SBN nanocrystals with various components ($x = 0.2$, 0.4, 0.6, and 0.8) at a reaction temperature of 1100°C for 3 h. The SBN20 nanocrystals possess the smallest size. Figure 2 indicates different morphologies of the SBN60 nanocrystals at different reaction temperatures (T = 950°C, 1000°C, 1050°C, and 1100°C) for 3 h. The grain size is determined by the annealing temperature and the SBN60 nanocrystals at a reaction temperature of 950°C get a smaller size. The XRD patterns for the nanocrystals obtained are shown in Figures 3 and 4. All peaks are assigned to SBN nanocrystals with a tetragonal tungsten-bronze (TB)

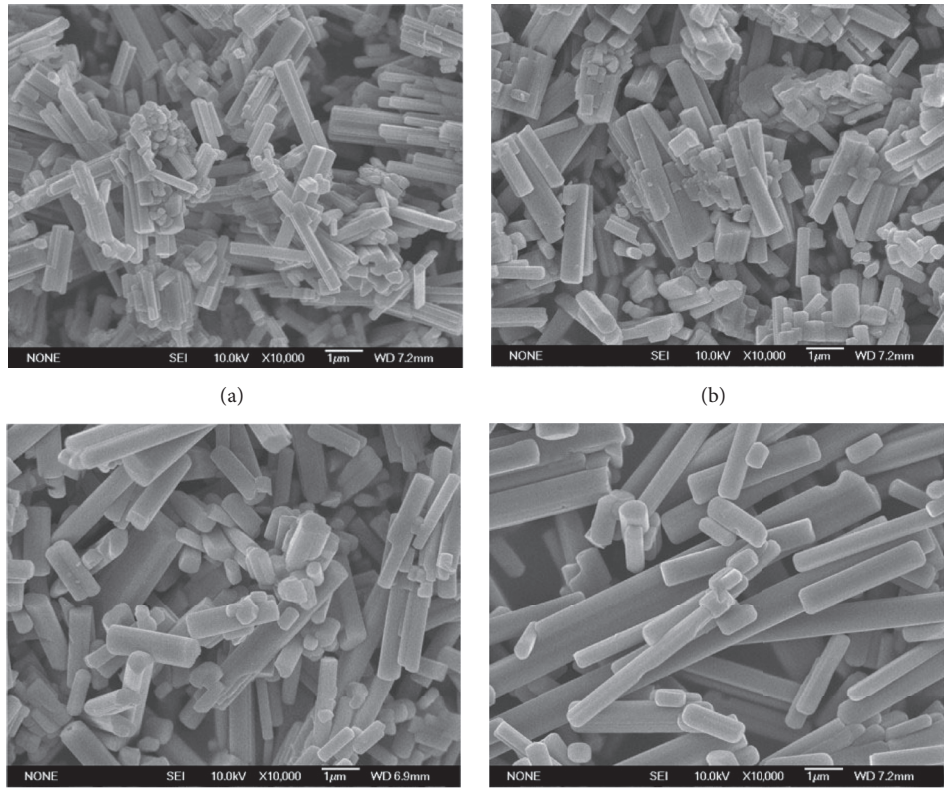

Figure 2: SEM images of the flux-synthesized SBN60 nanocrystals with flux-to-reactant weight ratio of 2 : 1 at different reaction temperatures for 3 h: (a) 950°C, (b) 1000°C, (c) 1050°C, and (d) 1100°C.

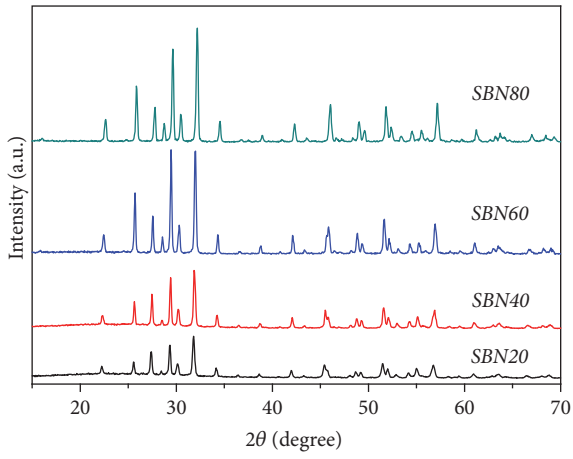

Figure 3: XRD patterns of the flux-synthesized SBN nanocrystals with flux-to-reactant weight ratio of 2 : 1 at a reaction temperature of 1100°C for 3 h.

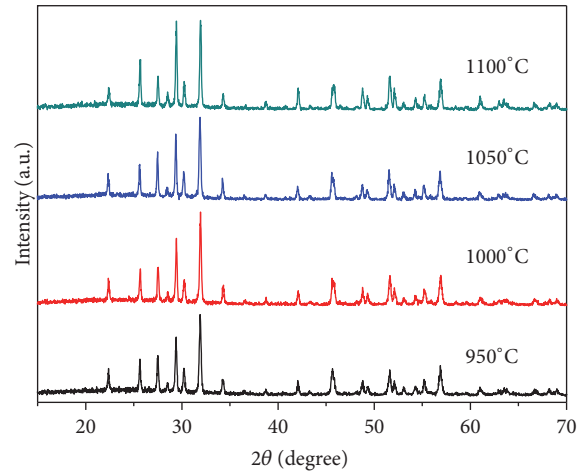

Figure 4: XRD patterns of the flux-synthesized SBN60 nanocrystals with flux-to-reactant weight ratio of 2 : 1 at different reaction temperatures for 3 h.

structure. The tested results confirm that all SBN nanocrystals are obtained randomly without having any impurity phase.

The SBN nanocrystals represent the similar absorption properties as observed from UV-vis DR spectra (Figure 5). Figure 5(a) indicates SBN nanocrystals with different components (x = 0.2, 0.4, 0.6, and 0.8) possess similar UV-vis absorption properties. In pure SBN nanocrystals, the UV-vis near the absorption edge will create a pair of electron–hole excitons. The constraints of these excitons are

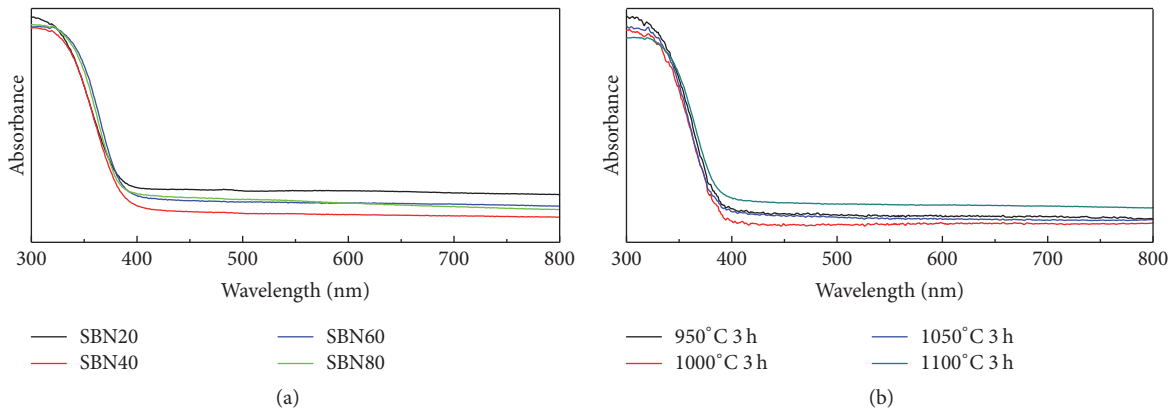

Figure 5: The UV-vis absorption spectra of the flux-synthesized SBN nanocrystals: (a) with different components; (b) at different reaction temperatures.

Table 1: Surface areas and photocatalytic rates for hydrogen production of the flux-prepared SBN nanocrystals.

Samples	Temperature/Dwelling time	Surface area [m^2/g]	Photocatalysis rate [μmol of $H_2 \cdot g^{-1} \cdot h^{-1}$]
SBN20	1100°C/3 h	3.8476	26.5
SBN40	1100°C/3 h	2.2028	56.2
SBN60	950°C/3 h	2.4400	122.35
SBN60	1000°C/3 h	2.4193	99.6
SBN60	1050°C/3 h	2.1549	102.1
SBN60	1100°C/3 h	1.7346	102.2
SBN80	1100°C/3 h	2.2127	79.55

weak and can be dissociated with the help of photons and phonons. The absorption edges of the SBN nanocrystals are at the wavelength region of approximate 390 nm and the band-gap of SBN crystal is about 3.18 eV at room temperature. So that UV-vis absorption properties are similar to different components. Simultaneously the reaction temperature of SBN nanocrystals has little effect on the UV-vis absorption nature as shown in Figure 5(b). Figure 5 also displays that the absorption edges of all kinds of SBN nanocrystals are at the same wavelength region of approximate 390 nm. The band-gap energy (E) can be calculated by the following equation [22]

$$E = \frac{1240}{\lambda}, \quad (1)$$

where λ is the wavelength in nanometers [23]. The calculated band-gap energy (E) corresponding to the 390 nm light wave is ~3.18 eV.

In metal-oxide photocatalysts, the light-driven excitation of electrons into their conduction bands can be used to drive the water splitting reactions for the reduction and oxidation of water to hydrogen and oxygen, respectively. The photocatalytic rates of SBN nanocrystals vary obviously with different components (x = 20, 40, 60, and 80) and reaction temperatures (T = 950°C, 1000°C, 1050°C, and 1100°C) as shown in Table 1. When the temperature of the sample is 1100°C, SBN60 has the highest photocatalytic efficiency. Table 1 indicates that the SBN60 nanocrystals exhibit stable photocatalytic rates for hydrogen production of ~100~130 μmol of $H_2 \cdot g^{-1} \cdot h^{-1}$ and especially the photocatalytic rate of SBN60 nanocrystals at a reaction temperature of 950°C gets the peak (122.35 μmol of $H_2 \cdot g^{-1} \cdot h^{-1}$). The structure of the SBN is nonfilled [1], so the photocatalytic rates can be controlled by changing the content of metal ions Sr and Ba in a large range. And the photocatalytic rates of SBN can be significantly improved by adjusting the Sr/Ba ratio in a certain range [24]. In the SBN nano-crystal structure, different positions are occupied by the metal ion, Sr and Ba. In addition, the radii of Sr and Ba ions are different. Therefore, the change of the composition leads to the distortion about the structure of the SBN. So different components have different UV-vis absorption properties and SBN60 has the highest photocatalytic efficiency. Table 1 also indicates that the surface area of SBN nanocrystals has little effect on the material photocatalytic activity. The surface area indicates one gram of the sample can be expanded at a certain temperature. The SBN nanocrystals with small size and powdered morphology display the higher photocatalytic rate. Especially the photocatalytic rate of SBN60 nanocrystals with the surface area of 2.4400 m^2/g gets the peak (122.35 μmol of $H_2 \cdot g^{-1} \cdot h^{-1}$). This is because the nanocrystals with small size and powered morphology are uniformly dispersed in the photocatalytic solution. They can absorb more light energy. So the photocatalytic rates of SBN nanocrystals can be controlled through changing the component and morphology of SBN nanocrystals, which are synthesized by using different experimental parameters.

4. Conclusions

The SBN nanocrystals are synthesized as single-crystal particles with sizes of ~100 nm~7 μm through changing component and reaction temperature. In order to gain some small nanocrystals with high surface area, the component and reaction temperature must be controlled properly. The absorption edges of the SBN nanocrystals are at the wavelength region of approximate 390 nm, which corresponds to band-gap energy of ~3.18 eV. Under UV light, the SBN60 nanocrystals exhibit excellent photocatalytic rates (~100~130 μmol/g/h of $H_2 \cdot g^{-1} \cdot h^{-1}$) in UV photocatalytic activity for water decomposition. The SBN60 nanocrystals synthesized at a reaction temperature of T = 950°C are found to possess highest photocatalytic rate (122.35 μmol of $H_2 \cdot g^{-1} \cdot h^{-1}$). The SBN nanocrystals with powdered morphology and small size display the higher photocatalytic rate. In a word, the water decomposition performance under UV mainly depends on the component and morphology of photocatalytic materials.

Conflicts of Interest

The authors declare that they have no conflicts of interest.

Acknowledgments

This work is financially supported by the National Natural Science Foundation of China (Grant no. 51205063), China Postdoctoral Science Foundation (Grant no. 2012M521281 and no. 2013T60643), and the Education Department Foundation of Fujian Province (Grant no. JA14032).

References

[1] W. C. Liu, A. D. Li, C. L. Mak, and K. H. Wongt, "Fabrication and electro-optic properties of ferroelectric nanocrystal/polymer composite films," *Journal of Physical Chemistry C*, vol. 112, no. 36, pp. 14202–14208, 2008.

[2] X. Y. Liu, Y. M. Liu, S. Takekawa, K. Kitamura, F. S. Ohuchi, and J. Y. Li, "Nanopolar structures and local ferroelectricity of Sr0.61Ba 0.39Nb2O6 relaxor crystal across Curie temperature by piezoresponse force microscopy," *Journal of Applied Physics*, vol. 106, no. 12, Article ID 124106, 2009.

[3] N. Ortega, P. Bhattacharya, and R. S. Katiyar, "Enhanced ferroelectric properties of multilayer SrBi2Ta2O9/SrBi2Nb 2O9 thin films for NVRAM applications," *Materials Science and Engineering B: Solid-State Materials for Advanced Technology*, vol. 130, no. 1-3, pp. 36–40, 2006.

[4] J. A. Bock, "Investigation of reduced $(Sr_xBa_{1-x})Nb_2O_6$ as a ferroelectric-based thermoelectric," *Materials Science and Engineering*, pp. 1–198, 2016.

[5] W. Horn, J. V. Bassewitz, and C. Denz, "Slow and fast light in photorefractive SBN:60," *Journal of Optics*, vol. 12, no. 10, Article ID 104011, 2010.

[6] J. Nuja, C. S. Suchand Sandeep, P. Reji, and K. Nandakumar, "Nonlinear optical properties of nanosized rare-earth-doped strontium barium niobate ceramics," *Spectroscopy Letters*, vol. 44, no. 5, pp. 334–339, 2011.

[7] S. Lee, R. H. T. Wilke, S. Trolier-Mckinstry, S. Zhang, and C. A. Randall, "SrxBa1-x Nb2 O6-δ Ferroelectric- thermoelectrics: Crystal anisotropy, conduction mechanism, and power factor," *Applied Physics Letters*, vol. 96, no. 3, Article ID 031910, 2010.

[8] T. Yamazawa, T. Honma, H. Suematsu, and T. Komatsu, "Synthesis, ferroelectric and electrooptic properties of transparent crystallized glasses with SrxBa1-xNb2O 6 nanocrystals," *Journal of the American Ceramic Society*, vol. 92, no. 12, pp. 2924–2930, 2009.

[9] A. Ando, M. Kimura, T. Minamikawa, and Y. Sakabe, "Layered piezoelectric ceramics for fine-tolerance resonator applications," *International Journal of Applied Ceramic Technology*, vol. 2, no. 1, pp. 33–44, 2005.

[10] Y. Yang, Y. Liu, B. Dou, X. Hao, and X. Liu, "Preparation and characterization of SBN50 ceramic powder by the combustion synthesis," *Ferroelectrics*, vol. 334, no. 1, pp. 97–103, 2006.

[11] P. M. Rorvik, T. Grande, and M. A. Einarsrud, "One-dimensional nanostructures of ferroelectric perovskites," *Advanced Materials*, vol. 23, no. 35, pp. 4007–4034, 2011.

[12] B. Yang, F. Li, J. P. Han et al., "Structural, dielectric and optical properties of barium strontium sodium niobate (Sr0.7Ba0.3)2NaNb5Oi 15 single crystals," *Journal of Physics D: Applied Physics*, vol. 37, no. 6, pp. 921–924, 2004.

[13] S.-I. Kang, J.-H. Lee, J.-J. Kim, H. Y. Lee, and S.-H. Cho, "Effect of sintering atmosphere on densification and dielectric characteristics in Sr0.5Ba0.5Nb2O6 ceramics," *Journal of the European Ceramic Society*, vol. 24, no. 6, pp. 1031–1035, 2004.

[14] C. M. Rouleau, G. E. Jellison Jr., and D. B. Beach, "Influence of MgO substrate miscut on domain structure of pulsed laser deposited SrxBa1-xNb2O6 as characterized by x-ray diffraction and spectroscopic ellipsometry," *Applied Physics Letters*, vol. 82, no. 18, pp. 2990–2992, 2003.

[15] I. S. Kim, S.-I. Kim, and Y. T. Kim, "Improvement of ferroelectric properties of Pt-SrBi2Nb2O9-SiO2-Si gate structure through oxygen plasma rapid thermal annealing," *Physica Status Solidi (A) Applied Research*, vol. 201, no. 1, pp. 125–129, 2004.

[16] X.-H. Wang, H. Gu, Q.-W. Huang, and M. Čeh, "Cation occupancy at the A1/A2 sites in strontium barium niobate microcrystals grown from molten NaCl and KCl salts," *Acta Materialia*, vol. 55, no. 16, pp. 5304–5309, 2007.

[17] A. Ratnamala, G. Suresh, V. D. Kumari, and M. Subrahmanyam, "Template synthesized nano-crystalline natrotantite: Preparation and photocatalytic activity for water decomposition," *Materials Chemistry & Physics*, vol. 110, no. 1, pp. 176–179, 2008.

[18] F. E. Osterloh, "Inorganic materials as catalysts for photochemical splitting of water," *Chemistry of Materials*, vol. 20, no. 1, pp. 35–54, 2008.

[19] A. Kudo, H. Kato, and S. Nakagawa, "Water splitting into H_2 and O_2 on new $Sr_2M_2O_7$ (M = Nb and Ta) photocatalysts with layered perovskite structures: factors affecting the photocatalytic activity," *Journal of Physical Chemistry*, vol. 104, no. 3, pp. 571–575, 2000.

[20] N. McLamb, P. P. Sahoo, L. Fuoco, and P. A. Maggard, "Flux growth of single-crystal $Na_2Ta_4O_{11}$ particles and their photocatalytic hydrogen production," *Crystal Growth & Design*, vol. 13, no. 6, pp. 2322–2326, 2013.

[21] F. Ciesielczyk, W. Szczekocka, K. Siwińska-Stefańska, A. Piasecki, and D. Paukszta, "Evaluation of the photocatalytic ability of a sol-gel-derived MgO-ZrO_2 oxide material," *Open Chemistry*, vol. 15, no. 1, pp. 7–18, 2017.

[22] M. Pudukudy, A. Hetieqa, and Z. Yaakob, "Synthesis, characterization and photocatalytic activity of annealingdependent quasi spherical and capsule like ZnO nanostructures," *Applied Surface Science*, vol. 319, no. 1, pp. 221–229, 2014.

[23] Z. Liu, W. Xu, J. Fang et al., "Decoration of BiOI quantum size nanoparticles with reduced graphene oxide in enhanced visible-light-driven photocatalytic studies," *Applied Surface Science*, vol. 259, pp. 441–447, 2012.

[24] C. Shekhar Pandey, J. Schreuer, M. Burianek, and M. Mühlberg, "Relaxor behavior of ferroelectric Ca0.22Sr0.12Ba 0.66Nb2O6," *Applied Physics Letters*, vol. 102, no. 2, Article ID 022903, 2013.